A compact cell-centered Galerkin method with subgrid stabilization

Daniele Antonio Di Pietro

A compact cell-centered Galerkin method with subgrid stabilization

Daniele A. Di Pietro

IFP, 1 & 4 avenue de bois Préau, 92852 Rueil-Malmaison Cedex, France

Abstract

In this work we propose a compact cell-centered Galerkin method with subgrid stabilization for anisotropic heterogeneous diffusion problems on general meshes. Both essential theoretical results and numerical validation are provided.

Résumé

Une méthode de Galerkine centrée aux mailles avec stencil compact et stabilisation de sous-grille. On propose une méthode de Galerkine centrée aux mailles avec stencil compact et stabilisation de sous-grille pour des problèmes de diffusion anisotrope et hétérogène. On présente à la fois les résultats théoriques essentiels et une validation numérique.

1. Introduction

Soit $\Omega \subset \mathbb{R}^d$, $d \geq 1$, un ouvert polyhédrique borné. On considère le problème modèle suivant :

$$-\nabla\cdot(\boldsymbol{\kappa}\nabla u) = f \text{ dans } \Omega, \qquad u = 0 \text{ sur } \partial\Omega, \tag{1}$$

où $f \in L^2(\Omega)$ et $\boldsymbol{\kappa}$ est un champ de diffusion tensoriel symétrique uniformement défini positif et constant par morceaux sur Ω. En posant $V \stackrel{\text{def}}{=} H^1_0(\Omega)$, la formulation faible de (1) s'écrit

$$\text{Trouver } u \in V \text{ t.q. } \int_\Omega \boldsymbol{\kappa}\nabla u\cdot\nabla v = \int_\Omega fv \text{ pour tout } v \in V. \tag{2}$$

La discrétisation de (1) par des méthodes de bas ordre sur des maillages généraux qui soient robustes par rapport à l'hétérogeneité et à l'anisotropie du tenseur de diffusion $\boldsymbol{\kappa}$, et qui aient en même temps des bonnes proprietés de stabilité est un sujet actif de recherche. Les méthodes de volumes finis classiques réposent sur des bilans par maille faisant intervenir des *flux numériques*. L'idée d'obtenir des flux numériques à l'aide une reconstruction locale peut être attribuée à Aavatsmark *et al.* et à Edwards *et al.* (voir, respectivement, [1] et [6] pour une bibliographie). Le problème principal de ces méthodes est qu'il

Email address: daniele-antonio.di-pietro@ifp.fr (Daniele A. Di Pietro).

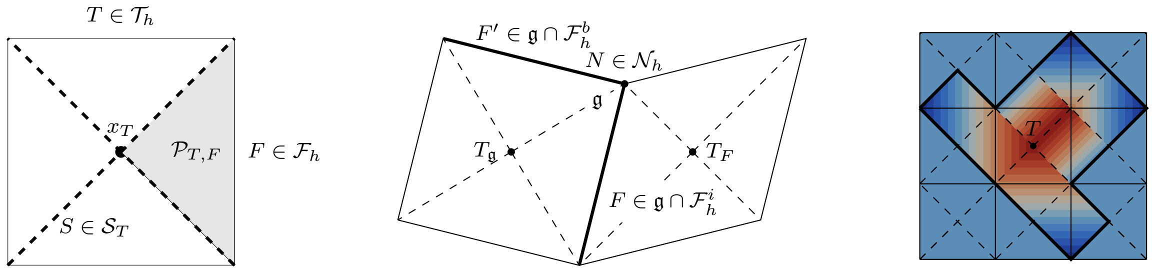

(a) Notation for the submesh (b) Notation for an L-group $\mathfrak{g}$ (in thick line) (c) Basis function φ_T

Figure 1. *Panels (a) and (b).* Notation *Panel (c).* An example of actual basis function $\varphi_T = \mathcal{I}_h(\mathbf{e}_T)$ for the space V_h of (3) on a 3×3 quadrangular mesh. Observe that $\text{supp}(\varphi_T)$ (thick line) is comprised between the maximal and minimal supports depicted on the left of Figure 2(a). It can also be appreciated that φ_T is continuous across the faces of T.

n'existe souvent pas de conditions simples à vérifier qui en garantissent la stabilité. Plus récemment, des approches variationnelles ont été proposées dans [7]. Les méthodes de ce type sont inconditionnellement coercives au prix d'un stencil élargi. De plus, elles ne sont définies qu'au niveau discret, ce qui ne permet pas d'appliquer les techniques d'analyse typiques des méthodes de Galerkine/éléments finis. L'analyse de convergence repose alors sur un argument de compacité, qui ne fournit pas une estimation de l'ordre de convergence [2, 7]. Une alternative a été suggéré dans [4], où on propose une famille de méthodes variationnelles centrées aux mailles dites *cell-centered Galerkin* (ccG), et basées sur des espaces polynomiaux par morceaux incomplets. Ces méthodes sont inconditionnellement coercives, et il est possible d'étendre la forme bilinéaire à un espace contenant la solution exacte. L'analyse de convergence se fait alors dans l'esprit du Lemme de Céa. Le desavantage principal de la famille de méthodes ccG de [4] consiste à avoir un stencil élargi, comparable à celui de [7]. Dans cette note, on propose une variation qui réduit significativement le stencil tout en gardant les bonnes propriétés de la méthode originale (coercivité inconditionnnelle, robustesse par rapport à l'hétérogeneité et à l'anisotropie de $\boldsymbol{\kappa}$). L'idée est de réduire le support des fonctions de base de l'espace discret en introduisant une reconstruction opportune sur une sous-grille. La consistance et la symétrie sont garanties par des termes de bord controlés par une stabilisation aux sous-faces. Dans les codes industriels (parallèles, $d = 3$), un stencil compact est crucial non seulement pour réduire l'occupation en mémoire, mais aussi pour minimiser les échanges de messages entre processeurs. En outre, vitesse de calcul et robustesse sont souvent faites passer avant la précision.

2. Discrete setting

Notation. The discretization of problem (2) is based on general polygonal meshes. In the context of the h-convergence analysis, we denote by $\mathcal{H} \subset \mathbb{R}_+^*$ a countable set having 0 as its unique accumulation point, and we adopt the concept of *admissible mesh sequence* $(\mathcal{T}_h)_{h\in\mathcal{H}}$ introduced in [2, Definition 2.1] (which may be consulted for further details on the regularity assumptions). We briefly recall here the relevant notations. For a given meshsize $h \in \mathcal{H}$, $\mathcal{T}_h = \{T\}$ denotes a partition of Ω into polygonal elements whose faces are portions of hyperplanes and such that $\boldsymbol{\kappa}$ *is constant inside each element*. The set of mesh vertices is denoted by $\mathcal{N}_h$. An *interface* is a portion of hyperplane $F \subset \partial T_1 \cap \partial T_2$, $T_1, T_2 \in \mathcal{T}_h$, with arbitrary but fixed unit normal $\mathbf{n}_F$, whereas a *boundary face* is a portion of hyperplane $F \subset \partial T \cap \partial\Omega$ with $T \in \mathcal{T}_h$ and outward normal $\mathbf{n}_F$. Interfaces are collected in the set $\mathcal{F}_h^i$, boundary faces in $\mathcal{F}_h^b$. We additionally set $\mathcal{F}_h \stackrel{\text{def}}{=} \mathcal{F}_h^i \cup \mathcal{F}_h^b$ and, for all $T \in \mathcal{T}_h$, $\mathcal{F}_T \stackrel{\text{def}}{=} \{F \in \mathcal{F}_h \mid F \subset \partial T\}$; conversely, we let $\mathcal{T}_F \stackrel{\text{def}}{=} \{T \in \mathcal{T}_h \mid F \subset \partial T\}$. The set of cells and faces sharing one vertex $N \in \mathcal{N}_h$ are respectively denoted by $\mathcal{T}_N$ and $\mathcal{F}_N$. For each $T \in \mathcal{T}_h$ we assume that there exists $\mathbf{x}_T \in T$ (the *cell-center*) such that T is star-shaped with respect to $\mathbf{x}_T$. For all $F \in \mathcal{F}_T$ we let $d_{T,F} \stackrel{\text{def}}{=} \text{dist}(\mathbf{x}_T, F)$, and we assume that $d_{T,F}$ is comparable to the face diameter h_F. For all $F \in \mathcal{F}_T$, $\mathcal{P}_{T,F}$ denotes the F-based pyramid of apex $\mathbf{x}_T$, i.e.

$$\forall T \in \mathcal{T}_h, \forall F \in \mathcal{F}_T, \qquad \mathcal{P}_{T,F} \stackrel{\text{def}}{=} \{\mathbf{x} \in T \mid \exists \mathbf{y} \in F, \exists \theta \in [0,1] \text{ such that } \mathbf{x} = \theta \mathbf{x}_T + (1-\theta)\mathbf{y}\}.$$

The subgrid obtained from the decomposition of the elements of $\mathcal{T}_h$ into pyramids is denoted by $\mathcal{S}_h$, i.e. $\mathcal{S}_h = \{\mathcal{P}_{T,F}\}_{T\in\mathcal{T}_h, F\in\mathcal{F}_T}$ (notation exemplified in Figure 1(a)). The set of lateral pyramid faces (*subfaces*) included in T is denoted by $\mathcal{S}_T$. For all $S \in \mathcal{S}_T$, $T \in \mathcal{T}_h$, we fix a unit normal $\mathbf{n}_S$ and let, for all $\varphi \in H^1(\mathcal{S}_h) \stackrel{\text{def}}{=} \{v \in L^2(\Omega) \mid \forall T \in \mathcal{T}_h, \forall F \in \mathcal{F}_T, v|_{\mathcal{P}_{T,F}} \in H^1(\mathcal{P}_{T,F})\}$,

$$[\![\varphi]\!] \stackrel{\text{def}}{=} \varphi^- - \varphi^+, \qquad \{\varphi\} \stackrel{\text{def}}{=} \tfrac{\varphi^- + \varphi^+}{2}, \qquad \varphi^{\pm}(\mathbf{x}) \stackrel{\text{def}}{=} \lim_{\epsilon\to 0^+} \varphi(\mathbf{x} \pm \epsilon \mathbf{n}_S) \text{ for a.e. } \mathbf{x} \in S.$$

The diameter of a subface $S \in \mathcal{S}_T$, $T \in \mathcal{T}_h$, is denoted by h_S. We introduce the following notation for the diffusion in the normal direction on faces and subfaces: For all $T \in \mathcal{T}_h$,

$$\text{for all } F \in \mathcal{F}_T,\ \lambda_F^T \stackrel{\text{def}}{=} \boldsymbol{\kappa}|_T \mathbf{n}_F \cdot \mathbf{n}_F \text{ and for all } S \in \mathcal{S}_T,\ \lambda_S \stackrel{\text{def}}{=} \boldsymbol{\kappa}|_T \mathbf{n}_S \cdot \mathbf{n}_S.$$

For boundary faces we shall simply write λ_F to alleviate the notation. Finally, the space of the cell-centered unknowns is denoted by $\mathbb{R}^{\mathcal{T}_h}$, and we use the notation $\mathbf{v}_h = (v_T)_{T\in\mathcal{T}_h} \in \mathbb{R}^{\mathcal{T}_h}$.

The L-reconstruction. The L-reconstruction of [1] is the main ingredient to design the incomplete polynomial space. We recall here the basics and refer to [2, §3.1] for a comprehensive presentation. Define the set of *L-groups* as in [2, Definition 3.1],

$$\mathcal{G} \stackrel{\text{def}}{=} \{\mathfrak{g} \subset \mathcal{F}_T \cap \mathcal{F}_N \mid T \in \mathcal{T}_N,\ N \in \mathcal{N}_h,\ \text{card}(\mathfrak{g}) = d\}.$$

For every $\mathfrak{g} \in \mathcal{G}$, we define the set of L-group cells $\mathcal{T}_\mathfrak{g} \stackrel{\text{def}}{=} \bigcup_{F\in\mathfrak{g}} \mathcal{T}_F$, among which we identify a cell $T_\mathfrak{g}$ such that $\mathfrak{g} \subset \mathcal{F}_{T_\mathfrak{g}}$ ($T_\mathfrak{g}$ may not be unique when concave elements are present); for all $F \in \mathfrak{g} \cap \mathcal{F}_h^i$, we denote by T_F the unique cell such that $F \subset \partial T_\mathfrak{g} \cap \partial T_F$ (the notation is exemplified in Figure 1(b)). For a given $\mathbf{v}_h \in \mathbb{R}^{\mathcal{T}_h}$ we construct the function $\xi^\mathfrak{g}_{\mathbf{v}_h}$ such that (i) $\xi^\mathfrak{g}_{\mathbf{v}_h}$ is affine inside every $\{\mathcal{P}_{T,F}\}_{F\in\mathfrak{g}, T\in\mathcal{T}_F}$ and $\xi^\mathfrak{g}_{\mathbf{v}_h}(\mathbf{x}_T) = v_T$ for all $T \in \mathcal{T}_\mathfrak{g}$; (ii) both $\xi^\mathfrak{g}_{\mathbf{v}_h}$ and its diffusive flux are continuous across group interfaces, i.e., for all $F \in \mathfrak{g} \cap \mathcal{F}_h^i$ and every $x \in F$,

$$\xi^\mathfrak{g}_{\mathbf{v}_h}|_{\mathcal{P}_{T_\mathfrak{g},F}}(x) = \xi^\mathfrak{g}_{\mathbf{v}_h}|_{\mathcal{P}_{T_F,F}}(x) \text{ and } (\boldsymbol{\kappa}\nabla\xi^\mathfrak{g}_{\mathbf{v}_h})|_{\mathcal{P}_{T_\mathfrak{g},F}}(x)\cdot\mathbf{n}_F = (\boldsymbol{\kappa}\nabla\xi^\mathfrak{g}_{\mathbf{v}_h})|_{\mathcal{P}_{T_F,F}}(x)\cdot\mathbf{n}_F.$$

(iii) for all $F \in \mathfrak{g} \cap \mathcal{F}_h^b$, $\xi^\mathfrak{g}_{\mathbf{v}_h}(\overline{\mathbf{x}}_F) = 0$ with $\overline{\mathbf{x}}_F \stackrel{\text{def}}{=} \int_F x/|F|_{d-1}$. It has been proved in [1] that $\xi^\mathfrak{g}_{\mathbf{v}_h}$ only depends on the values $(v_T)_{T\in\mathcal{T}_\mathfrak{g}}$. In particular, it is inferred from [2, Lemma 3.1] that, for all $F \in \mathfrak{g}$ there holds $\xi^\mathfrak{g}_{\mathbf{v}_h}|_{\mathcal{P}_{T_\mathfrak{g},F}}(\mathbf{x}) = v_{T_\mathfrak{g}} + \nabla\xi^\mathfrak{g}_{\mathbf{v}_h}|_{\mathcal{P}_{T_\mathfrak{g},F}}\cdot(\mathbf{x} - \mathbf{x}_{T_\mathfrak{g}})$ where $\nabla\xi^\mathfrak{g}_{\mathbf{v}_h}|_{\mathcal{P}_{T_\mathfrak{g},F}} = \mathbf{A}_\mathfrak{g}^{-1}\mathbf{b}(\mathbf{v}_h)$ with matrix $\mathbf{A}_\mathfrak{g} \in \mathbb{R}^{d,d}$ and linear d-valued application $\mathbf{b}_\mathfrak{g} : \mathbb{R}^{\mathcal{T}_h} \to \mathbb{R}^d$ given by

$$\mathbf{A}_\mathfrak{g} \stackrel{\text{def}}{=} \begin{bmatrix} \left(\lambda_F^{T_F} d_{T_F,F}^{-1}(\mathbf{x}_{T_F} - \mathbf{x}_{T_\mathfrak{g}}) + (\boldsymbol{\kappa}_{T_\mathfrak{g}} - \boldsymbol{\kappa}_{T_F})\mathbf{n}_{T_\mathfrak{g},F}\right)^t_{F\in\mathfrak{g}\cap\mathcal{F}_h^i} \\ \left(\lambda_F d_{T_\mathfrak{g},F}^{-1}(\overline{\mathbf{x}}_F - \mathbf{x}_{T_\mathfrak{g}})\right)^t_{F\in\mathfrak{g}\cap\mathcal{F}_h^b} \end{bmatrix}, \quad \mathbf{b}_\mathfrak{g}(\mathbf{v}_h) \stackrel{\text{def}}{=} \begin{bmatrix} \left(\lambda_F^{T_F} d_{T_F,F}^{-1}(v_{T_F} - v_{T_\mathfrak{g}})\right)_{F\in\mathfrak{g}\cap\mathcal{F}_h^i} \\ \left(-\lambda_F d_{T_\mathfrak{g},F}^{-1} v_{T_\mathfrak{g}}\right)_{F\in\mathfrak{g}\cap\mathcal{F}_h^b} \end{bmatrix}.$$

(The cell and face centers and the normals are intended as column vectors, and $\mathbf{A}_\mathfrak{g}$ is defined by row blocks; $\mathbf{n}_{T_\mathfrak{g},F}$ denotes the normal to F pointing out of $T_\mathfrak{g}$). When $d = 1$, $\nabla\xi^\mathfrak{g}_{\mathbf{v}_h}|_{\mathcal{P}_{T_\mathfrak{g},F}}$ coincides with the classical two-point gradient. Sufficient conditions for the inversibility of $\mathbf{A}_\mathfrak{g}$ are proposed in [2]; in particular, whenever $\boldsymbol{\kappa}$ is homogeneous, a sufficient condition is that the cell-centers $(\mathbf{x}_T)_{T\in\mathcal{T}_\mathfrak{g}}$ form a non-degenerate simplex. Finally, for all $F \in \mathfrak{g} \cap \mathcal{F}_h^i$, an explicit expression for $\xi^\mathfrak{g}_{\mathbf{v}_h}|_{\mathcal{P}_{T_F,F}}$ can also be derived (see again [2, Lemma 3.1]).

The discrete functional space. The procedure outlined in the previous section allows to reconstruct a piecewise affine field on $\mathcal{S}_h$ that is continuous across interfaces and has continuous diffusive fluxes. Let $\mathbb{P}_d^k(\mathcal{S}_h)$ denote the space of broken polynomial functions on $\mathcal{S}_h$ of total degree at most k. We *assume*

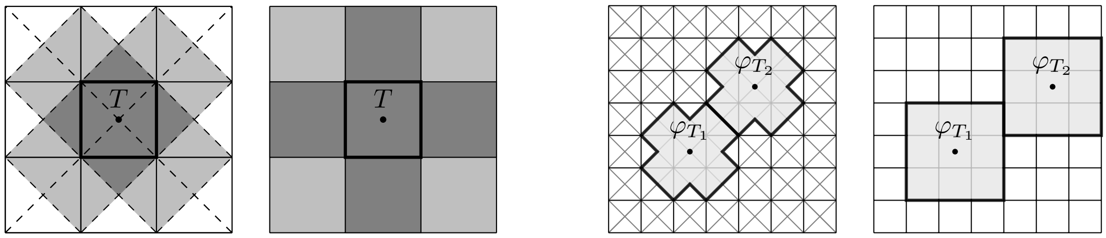

(a) Minimal (dark) and maximal (light+dark) support for $\varphi = \mathcal{I}_h(\mathbf{e}_T)$ (cell T in bold line). *Left.* Proposed method *Right.* Method of [4]

(b) Worst-case interacting cells for maximally supported φ_{T_1} and φ_{T_2}. *Left.* Proposed method *Right.* Method of [4]

Figure 2. Stencil reduction related to the more compact support of basis functions with respect to the method of [4]. *Panel (a).* $\mathcal{T}_h$=quadrangular 3×3 mesh *Panel (b).* $\mathcal{T}_h$=quadrangular 7×7 mesh, supports in shades of gray

that the sets $\mathcal{G}_F \stackrel{\text{def}}{=} \{\mathfrak{g} \in \mathcal{G} \mid F \subset \mathfrak{g} \text{ and } \mathbf{A}_{\mathfrak{g}} \text{ is invertible}\}$ are non empty for all $F \in \mathcal{F}_h$. For each $F \in \mathcal{F}_h$, we select the L-group $\mathfrak{g}_F \in \mathcal{G}_F$ for which $\|\mathbf{A}_{\mathfrak{g}_F}^{-1}\|_\infty$ is the smallest (see [2, eq. (B.9)]), and let $\mathcal{I}_h \in \mathcal{L}(\mathbb{R}^{\mathcal{T}_h}, \mathbb{P}_d^1(\mathcal{S}_h))$ realize the mapping $\mathbb{R}^{\mathcal{T}_h} \ni \mathbf{v}_h \mapsto \mathcal{I}_h(\mathbf{v}_h) \in \mathbb{P}_d^1(\mathcal{S}_h)$ with

$$\forall T \in \mathcal{T}_h, \forall F \in \mathcal{F}_T, \qquad \mathcal{I}_h(\mathbf{v}_h)|_{\mathcal{P}_{T,F}} = \xi_{\mathbf{v}_h}^{\mathfrak{g}_F}|_{\mathcal{P}_{T,F}}.$$

The injectivity of $\mathcal{I}_h$ follows from the non-emptiness of the sets $\{\mathcal{G}_F\}_{F \in \mathcal{F}_h}$ together with the fact that every $T \in \mathcal{T}_h$ appears in at least one local reconstruction. Drawing on the ideas of [4], we set

$$V_h \stackrel{\text{def}}{=} \mathcal{I}_h(\mathbb{R}^{\mathcal{T}_h}) \subset \mathbb{P}_d^1(\mathcal{S}_h). \tag{3}$$

A bijective operator can be obtained restricting the co-domain of $\mathcal{I}_h$ to V_h. Observe that the functions in V_h are continuous across mesh interfaces but they can jump across subfaces, as depicted in Figure 1(c). Choose $\{\varphi_T \stackrel{\text{def}}{=} \mathcal{I}_h(\mathbf{e}_T)\}_{T \in \mathcal{T}_h}$ as basis for V_h ($\mathbf{e}_T$ being the Tth vector of the canonical basis of $\mathbb{R}^{\mathcal{T}_h}$; other choices leading to further stencil reduction will be discussed in a separate work). The reduced stencil with respect to the original ccG method of [4] follows from the more compact support of the basis functions, which reduces cell interactions. The actual support of each basis function φ_T varies according to the specific choices for $\{\mathfrak{g}_F\}_{F \in \mathcal{F}_T}$, but we can identify minimal and maximal supports (see Figure 2). Let

$$V_\dagger \stackrel{\text{def}}{=} \left\{ v \in V \cap H^2(\mathcal{S}_h) \mid \forall F \subset \partial T_1 \cap \partial T_2,\, (\boldsymbol{\kappa}\nabla v)|_{T_1}\cdot\mathbf{n}_F = (\boldsymbol{\kappa}\nabla v)|_{T_2}\cdot\mathbf{n}_F \right\}$$

and set $V_{\dagger h} \stackrel{\text{def}}{=} V_\dagger + V_h$ (the additional local regularity in $V_\dagger$ is required to extend the discrete bilinear form on a space containing the exact solution). As common in dG methods, we denote by ∇_h the broken gradient operator on $\mathcal{S}_h$. The discrete bilinear form is defined on $V_{\dagger h} \times V_h$ as follows:

$$\begin{aligned} a_h(w, v_h) \stackrel{\text{def}}{=} &\int_\Omega \boldsymbol{\kappa}\nabla_h w\cdot\nabla_h v_h - \sum_{F \in \mathcal{F}_h^b} \int_F [(\boldsymbol{\kappa}\nabla w\cdot\mathbf{n}_F)v_h + (\boldsymbol{\kappa}\nabla v_h\cdot\mathbf{n}_F)w] + \sum_{F \in \mathcal{F}_h^b} \int_F \frac{\eta\lambda_F}{h_F} w v_h \\ &- \sum_{T \in \mathcal{T}_h} \sum_{S \in \mathcal{S}_T} \int_S (\boldsymbol{\kappa}\{\nabla_h w\}\cdot\mathbf{n}_S [\![v_h]\!] + \boldsymbol{\kappa}\{\nabla_h v_h\}\cdot\mathbf{n}_S [\![w]\!]) + \sum_{T \in \mathcal{T}_h} \sum_{S \in \mathcal{S}_T} \int_S \frac{\eta\lambda_S}{h_S} [\![w]\!][\![v_h]\!]. \end{aligned} \tag{4}$$

The last term penalizes the jumps at subfaces; it is unnecessary to penalize the jumps at the faces of $\mathcal{T}_h$ since the functions in V_h are continuous across every interface (see Figure 1(c)). Owing to the subface and boundary terms, two basis functions whose support shares at least one subface interact, thereby contributing to the stencil of the method (see Figure 2(b)). All integrals in the expression of a_h can be evaluated using the center of mass as a quadrature node. The discrete problem reads

$$\text{Find } u_h \in V_h \text{ such that } a_h(u_h, v_h) = \int_\Omega f v_h \text{ for all } v_h \in V_h. \tag{5}$$

Basic error estimate. We now identify some relevant properties of the bilinear form a_h. To prove coercivity, we equip the space V_h with the energy norm

$$|||v_h|||^2 \stackrel{\text{def}}{=} \|\boldsymbol{\kappa}^{1/2}\nabla_h v_h\|^2_{[L^2(\Omega)]^d} + \sum_{T\in\mathcal{T}_h}\sum_{S\in\mathcal{S}_T} \frac{\lambda_S}{h_S}\|[\![v_h]\!]\|^2_{L^2(S)} + \sum_{F\in\mathcal{F}_h^b} \frac{\lambda_F}{h_F}\|v_h\|^2_{L^2(F)}.$$

To prove the boundedness of a_h, we introduce the following extended norm on $V_{\dagger h}$: For all $v \in V_{\dagger h}$,

$$|||v|||^2_* \stackrel{\text{def}}{=} |||v|||^2 + \sum_{T\in\mathcal{T}_h}\sum_{S\in\mathcal{S}_T} h_S\|\boldsymbol{\kappa}^{1/2}\{\nabla_h v\}\cdot\mathbf{n}_S\|^2_{L^2(S)} + \sum_{F\in\mathcal{F}_h^b} h_F\|\boldsymbol{\kappa}^{1/2}\nabla v\cdot\mathbf{n}_F\|^2_{L^2(F)}.$$

The $|||\cdot|||$-norm and the $|||\cdot|||_*$-norm are uniformly equivalent on V_h. The bilinear form a_h enjoys the following properties: (i) *Consistency.* Let u solve (2) and additionally assume that $u \in V_\dagger$. Then, for all $v_h \in V_h$, $a_h(u, v_h) = \int_\Omega f v_h$. (ii) *Coercivity.* For all $\eta > \underline{\eta}$ (with $\underline{\eta}$ only depending on the mesh regularity), there exists $C_{\text{sta}}>0$ independent of both the meshsize h and of the diffusion field $\boldsymbol{\kappa}$ such that for all $v_h \in V_h$, $a_h(v_h, v_h) \geq C_{\text{sta}}|||v_h|||^2$. (iii) *Boundedness.* There exists C_{bnd} independent of both the meshsize h and of the diffusion field $\boldsymbol{\kappa}$ such that, for all $(w, v_h) \in V_{\dagger h} \times V_h$, $a_h(w, v_h) \leq C_{\text{bnd}}|||w|||_*|||v_h|||$. Using the above properties, the following error is classically inferred proceeding in the spirit of Céa's Lemma.

Theorem 1 (Error estimate) *Let u solve* (2) *and additionally assume that $u \in V_\dagger$. Then,*

$$|||u - u_h||| \leq \left(1 + C_{\text{bnd}}C_{\text{sta}}^{-1}\right) \inf_{w_h\in V_h} |||u - w_h|||_*.$$

The multiplicative constant in the right-hand side does not depend on the diffusion tensor, which renders the method robust with respect to both heterogeneity and anisotropy of $\boldsymbol{\kappa}$. First order convergence rate can be inferred if u belongs to the space of [2, Lemma 3.2] or $u \in H^2(\Omega)$ in the homogeneous case.

Convergence to minimal regularity solutions. Convergence to solutions that are barely in V can also be proved. The $|||\cdot|||$-norm satisfies a discrete Poincaré inequality on V_h (proceed as in [5, Theorem 6.1]). As a consequence, we have the uniform *a priori* estimate $|||u_h||| \leq \sigma_2 C_{\text{sta}}^{-1}\|f\|_{L^2(\Omega)}$ (σ_2 results from the discrete Poincaré inequality). In the spirit of [3], we define a discrete gradient that is weakly asymptotically consistent by introducing lifting operators. In particular, for all $T \in \mathcal{T}_h$, all $S \in \mathcal{S}_T$, $\mathrm{r}_S : L^2(S) \to [\mathbb{P}^0_d(\mathcal{S}_h)]^d$ is such that, for all $\varphi \in L^2(S)$, $\int_\Omega \mathrm{r}_S(\varphi)\cdot\tau_h = \int_S \varphi\{\tau_h\}\cdot\mathbf{n}_S$ for all $\tau_h \in [\mathbb{P}^0_d(\mathcal{S}_h)]^d$. Similarly, for all $F \in \mathcal{F}_h^b$ and all $\varphi \in L^2(F)$, $\mathrm{r}_F : L^2(F) \to [\mathbb{P}^0_d(\mathcal{S}_h)]^d$ is such that $\int_\Omega \mathrm{r}_F(\varphi)\cdot\tau_h = \int_F \varphi\tau_h\cdot\mathbf{n}_F$ for all $\tau_h \in [\mathbb{P}^0_d(\mathcal{S}_h)]^d$.

Lemma 2 (Discrete Rellich theorem) *Let $(v_h)_{h\in\mathcal{H}}$ be a sequence in $(V_h)_{h\in\mathcal{H}}$ uniformly bounded in the $|||\cdot|||$-norm and set, for all $v_h \in V_h$,*

$$\mathfrak{G}_h(v_h) \stackrel{\text{def}}{=} \nabla_h v_h - \sum_{T\in\mathcal{T}_h}\sum_{S\in\mathcal{S}_T} \mathrm{r}_S([\![v_h]\!]) - \sum_{F\in\mathcal{F}_h^b} \mathrm{r}_F(v_h) \stackrel{\text{def}}{=} \nabla_h v_h - \mathrm{R}_h(v_h).$$

Then, there exists $v_h \in H^1_0(\Omega)$ such that, up to a subsequence, $v_h \to v$ strongly in $L^2(\Omega)$ and $\mathfrak{G}_h(v_h) \rightharpoonup \nabla v$ weakly in $[L^2(\Omega)]^d$ (that is to say, $\mathfrak{G}_h$ is weakly asymptotically consistent*).*

To gradient $\mathfrak{G}_h$ is also strongly consistent for piecewise smooth functions with continuous diffusive fluxes belonging to the space of [2, Lemma 3.2]. The proof of Theorem 3 relies on the following equivalent form for a_h in $V_h \times V_h$:

$$a_h(u_h, v_h) = \int_\Omega \boldsymbol{\kappa}\mathfrak{G}_h(u_h)\cdot\mathfrak{G}_h(v_h) + j_h(u_h, v_h),$$

where $j_h(u_h, v_h) = -\int_\Omega \boldsymbol{\kappa}\,\mathrm{R}_h(u_h)\cdot\mathrm{R}_h(v_h) + \sum_{T\in\mathcal{T}_h}\sum_{S\in\mathcal{S}_T}\int_S \frac{\eta\lambda_S}{h_S}[\![u_h]\!][\![v_h]\!] + \sum_{F\in\mathcal{F}_h^b}\int_F \frac{\eta\lambda_F}{h_F}u_h v_h$.

Theorem 3 (Convergence to minimal regularity solutions) *Let $(u_h)_{h\in\mathcal{H}}$ denote the sequence of discrete solutions to* (5) *on the admissible mesh sequence $(\mathcal{T}_h)_{h\in\mathcal{H}}$, and let $u \in V$ solve* (2)*. Then, $u_h \to u$ strongly in $L^2(\Omega)$ and $\nabla_h u_h \to \nabla u$ strongly in $[L^2(\Omega)]^d$.*

Table 1
Comparison of the proposed method (top) with the original ccG method of [4] (bottom) on the heterogeneous test case (6) (left) and on the anisotropic test case (7) (right). The stencil is defined as the average number of nonzero element in a row.

card($\mathcal{T}_h$)	$\|u-u_h\|_{L^2(\Omega)}$	order	$\|\|\|u-u_h\|\|\|$	order	stencil
proposed method					
3584	1.3027e-03	–	4.5746e-02	–	15.03
14336	3.1039e-04	2.07	2.2608e-02	1.02	15.16
57344	8.6435e-05	1.84	1.1581e-02	0.97	15.22
229376	1.9971e-05	2.11	5.6241e-03	1.04	15.25
ccG method of [4]					
3584	5.2227e-04	–	2.8501e-02	–	25.26
14336	1.2926e-04	2.01	1.4194e-02	1.01	25.73
57344	3.2545e-05	1.99	7.1126e-03	1.00	26.11
229376	7.9803e-06	2.03	3.5293e-03	1.01	26.10

card($\mathcal{T}_h$)	$\|u-u_h\|_{L^2(\Omega)}$	order	$\|\|\|u-u_h\|\|\|$	order	stencil
proposed method					
806	6.2131e-03	–	9.0381e-02	–	14.69
3162	1.7417e-03	1.83	4.5942e-02	0.98	15.25
12632	5.7562e-04	1.60	2.2897e-02	1.00	15.38
50548	1.4492e-04	1.99	1.1341e-02	1.01	15.52
ccG method of [4]					
806	4.0093e-03	–	4.8250e-02	–	25.33
3162	1.7803e-03	1.17	2.7231e-02	0.83	26.35
12632	4.9217e-04	1.85	1.3674e-02	0.99	26.85
50548	1.3945e-04	1.82	6.9776e-03	0.97	27.12

3. Numerical validation

To assess the robustness with respect to the heterogeneity of $\boldsymbol{\kappa}$, consider the following pseudo two-dimensional exact solution to (2) on the unit square domain $\Omega = (0,1)^2$:

$$u = \begin{cases} -\frac{1}{2}x^2 + \frac{3+\epsilon}{4(1+\epsilon)}x & \text{if } x \leq \frac{1}{2}, \\ -\frac{1}{2\epsilon}x^2 + \frac{3+\epsilon}{4\epsilon(1+\epsilon)}x + \frac{\epsilon-1}{4\epsilon(1+\epsilon)} & \text{if } x > \frac{1}{2}. \end{cases} \qquad \boldsymbol{\kappa} = \begin{cases} 1 & \text{if } x < \frac{1}{2}, \\ \epsilon & \text{if } x > \frac{1}{2}, \end{cases} \qquad f = 1, \tag{6}$$

with heterogeneity ratio $\epsilon = 10^{-3}$. To evaluate the method with respect to the anisotropy of $\boldsymbol{\kappa}$, we consider the following exact solution on $\Omega = (0,1)^2$:

$$u = \sin(\pi x)\sin(\pi y), \qquad \kappa_{xx} = 1,\ \kappa_{xy} = \kappa_{yx} = 0,\ \kappa_{yy} = \epsilon, \tag{7}$$

with adapted right-hand side f and anisotropy ratio $\epsilon = 10^{-3}$. The results on non-structured triangular meshes are collected in Table 1. An inspection of the rightmost columns shows a significant stencil reduction in both cases for the proposed method. However, although both methods show the same formal order of convergence, a slight degradation of the precision is observed for the proposed method.

References

[1] I. Aavatsmark, G. T. Eigestad, B. T. Mallison, and J. M. Nordbotten. A compact multipoint flux approximation method with improved robustness. *Numer. Methods Partial Differential Equations*, 24(5):1329–1360, 2008.

[2] L. Agélas, D. A. Di Pietro, and J. Droniou. The G method for heterogeneous anisotropic diffusion on general meshes. *M2AN Math. Model. Numer. Anal.*, 2010. Published online.

[3] L. Agélas, D. A. Di Pietro, R. Eymard, and R. Masson. An abstract analysis framework for nonconforming approximations of diffusion problems on general meshes. *IJFV*, 7(1):1–29, 2010.

[4] D. A. Di Pietro. Cell centered Galerkin methods. *C. R. Math. Acad. Sci. Paris*, 348:31–34, 2010.

[5] D. A. Di Pietro and A. Ern. Discrete functional analysis tools for discontinuous Galerkin methods with application to the incompressible Navier-Stokes equations. *Math. Comp.*, 79:1303–1330, 2010.

[6] M. G. Edwards. Unstructured control-volume distributed full tensor finite volume schemes with flow based grids. *Comput. Geosci.*, 6:433–452, 2002.

[7] R. Eymard, Th. Gallouët, and R. Herbin. Discretization of heterogeneous and anisotropic diffusion problems on general nonconforming meshes SUSHI: a scheme using stabilization and hybrid interfaces. *IMA J. Numer. Anal.*, 2010. Published online.